DNA AND CELL BIOLOGY
Volume 00, Number 00, 2011

Pp. 1–12
DOI: 10.1089/dna.2011.1240

ORIGINAL RESEARCH ARTICLE

In vivo Safety and Antitumor Efficacy of Bifunctional Small Hairpin RNAs Specific for the Human Stathmin 1 Oncoprotein

Anagha P. Phadke,[1] Chris M. Jay,[1] Zhaohui Wang,[1] Salina Chen,[1] Shengnan Liu,[1,2] Courtney Haddock,[1] Padmasini Kumar,[1] Beena O. Pappen,[1] Donald D. Rao,[1] Nancy S. Templeton,[1] Egeenee Q. Daniels,[3] Craig Webb,[4] David Monsma,[4] Stephanie Scott,[4] Dawna Dylewski,[4] Hermann B. Frieboes,[5] Francis Charles Brunicardi,[6] Neil Senzer,[1,2,7,8] Phillip B. Maples,[1] John Nemunaitis,[1,2,7,8] and Alex W. Tong[1]

Bifunctional small hairpin RNAs (bi-shRNAs) are functional miRNA/siRNA composites that are optimized for posttranscriptional gene silencing through concurrent mRNA cleavage-dependent and -independent mechanisms (Rao *et al.*, 2010). We have generated a novel bi-shRNA using the miR30 scaffold that is highly effective for knockdown of human stathmin (STMN1) mRNA. STMN1 overexpression well documented in human solid cancers correlates with their poor prognosis. Transfection with the bi-shSTMN1–encoding expression plasmid (pbi-shSTMN1) markedly reduced CCL-247 human colorectal cancer and SK-Mel-28 melanoma cell growth *in vitro* (Rao *et al.*, 2010). We now examine *in vivo* the antitumor efficacy of this RNA interference-based approach with human tumor xenografted athymic mice. A single intratumoral (IT) injection of pbi-shSTMN1 (8 μg) reduced CCL-247 tumor xenograft growth by 44% at 7 days when delivered as a 1,2-dioleoyl-3-trimethylammoniopropane:cholesterol liposomal complex. Extended growth reductions (57% at day 15; $p < 0.05$) were achieved with three daily treatments of the same construct. STMN1 protein reduction was confirmed by immunoblot analysis. IT treatments with pbi-shSTMN1 similarly inhibited the growth of tumorgrafts derived from low-passage primary melanoma (≥70% reduction for 2 weeks) and abrogated osteosarcoma tumorgraft growth, with the mature bi-shRNA effector molecule detectable for up to 16 days after last injection. Antitumor efficacy was evident for up to 25 days posttreatment in the melanoma tumorgraft model. The maximum tolerated dose by IT injection of >92 μg (Human equivalent dose [HED] of >0.3 mg/kg) in CCL-247 tumor xenograft-bearing athymic mice was ~10-fold higher than the extrapolated IC_{50} of 9 μg (HED of 0.03 mg/kg). Healthy, immunocompetent rats were used as biorelevant models for systemic safety assessments. The observed maximum tolerated dose of <100 μg for intravenously injected pbi-shSTMN1 (mouse equivalent of <26.5 μg; HED of <0.09 mg/kg) confirmed systemic safety of the therapeutic dose, hence supporting early-phase assessments of clinical safety and preliminary efficacy.

Introduction

Stathmin 1 (STMN1) is a 17-kDa phosphoprotein that is necessary for cell cycle progression and mitosis. It belongs to a family of microtubule-destabilizing proteins with an important role in maintaining the steady phase of the cytoskeleton assembly (Rubin and Atweh, 2004). STMN1 is highly expressed in a variety of assessed human cancers, including acute leukemia, lymphoma, prostate cancer, breast cancer, head and neck cancer, and osteosarcoma, among others (Mistry and Atweh, 2002; Rubin and Atweh, 2004; Alli *et al.*, 2007b; Rana *et al.*, 2008). On the basis of a process of connectivity scoring to identify cancer-relevant and potentially critical molecular targets, we have identified *STMN1* as a candidate target gene among a group of differentially overexpressed mRNA and protein signal

[1]Gradalis, Inc., Dallas, Texas.
[2]Baylor Sammons Cancer Center, Dallas, Texas.
[3]Laboratory Animal Medicine, University of North Texas Health Science Center, Fort Worth, Texas.
[4]Van Andel Research Institute, Grand Rapids, Michigan.
[5]Department of Bioengineering, James Graham Brown Cancer Center, University of Louisville, Louisville, Kentucky.
[6]Michael E. DeBakey Department of Surgery, Baylor College of Medicine, Houston, Texas.
[7]Mary Crowley Cancer Research Centers, Dallas, Texas.
[8]Texas Oncology, Dallas, Texas.

couplets in >80% of 30 paired tumor versus normal tissues analyzed (Nemunaitis *et al.*, 2007). These findings are consistent with recent data that STMN1 overexpression is critical for maintenance and progression of malignant phenotypes in various human cancers including colorectal cancer, melanoma, and osteosarcoma (Zhang *et al.*, 2004; Alli *et al.*, 2007b), making STMN1 an attractive candidate for cancer-targeted biotherapy.

The effectiveness of STMN1-targeted approaches has been mostly examined *in vitro* by us (Rao *et al.*, 2010) and others (Zhang *et al.*, 2006; Wang *et al.*, 2007; Jiang *et al.*, 2009; Carney and Cassimeris, 2010; Gan *et al.*, 2010; Hsieh *et al.*, 2010; Jeon *et al.*, 2010) as singlet or combinational therapy with chemotherapeutic agents (Iancu *et al.*, 2000; Alli *et al.*, 2002; Mistry and Atweh, 2006; Mistry *et al.*, 2007; Wang *et al.*, 2007; Alli *et al.*, 2007a; Rayburn and Zhang, 2008; Vaishnaw *et al.*, 2010). On the basis of cumulative findings that STMN1 knockdown correspondingly inhibited human tumor cell growth, we have constructed a novel RNA interference (RNAi)–based therapeutic with bifunctional features. The bifunctional small hairpin RNA (bi-shRNA) comprises of two stem-loop structures encoded within the same expression construct. The transcribed mature effector small RNA molecules are endowed with separate posttranscriptional cleavage-dependent or -independent gene silencing functions. Using this bifunctional shRNA specific for STMN1 (pbi-shSTMN1), we have demonstrated effective STMN1 knockdown in human colorectal cancer CCL-247 cells, achieving significant tumor cell kill at enhanced potency (IC_{50} that was 5 log lower than molar equivalent of RNA oligonucleotides) and for a longer duration than previously described olignonucleotide-based approaches. Treated CCL-247 cells with a wild-type p53 phenotype (Liu and Bodmer, 2006; Olivier *et al.*, 2009) displayed cell-cycle arrest and subsequent apoptosis (Rao *et al.*, 2010). Increased STMN1 expression was associated with p53 mutation that contributed to enhanced tumorigenicity in hepatocellular carcinoma (Yuan *et al.*, 2006).

The present study assessed the *in vivo* efficacy of intratumoral (IT) pbi-shSTMN1 treatments, using immune-compromised mice bearing xenografts derived from established human cancer cell lines or low-passage primary human tumors. Additionally, safety of the pbi-shSTMN1-LP was assessed following a single intravenous (IV) injection in a biorelevant rat model. With an ultimate aim of achieving systemic cancer-selective delivery, studies were performed following encapsulation of the pbi-shSTMN1 in cationic liposomes composed of the biodegradable lipid 1,2-dioleoyl-3-trimethyl-ammoniopropane (DOTAP) and cholesterol (pbi-shSTMN1-LP). Cationic liposomes are one of the most commonly used nonviral vehicles for cancer therapeutics delivery (Templeton, 2002; Zhang *et al.*, 2007; Ashihara *et al.*, 2009) and known to prolong the retention time of plasmid DNA in tumors when compared with administration of naked DNA (Clark *et al.*, 2000; Nomura *et al.*, 1997). pbi-shSTMN1 plasmid was encapsulated in DOTAP:cholesterol liposomal formulation at a ratio of 50:45, previously shown to be highly effective for achieving gene expression of the plasmid DNA payload administered intramuscularly (Phadke *et al.*, 2009), intratumorally (Ramesh *et al.*, 2001; Templeton, 2002) or intravenously (Templeton *et al.*, 1997).

Materials and Methods

Plasmid DNA and preparation of lipoplexes

The pbi-shSTMN1 plasmid and the scrambled control plasmids were constructed as previously described (Phadke *et al.*, 2009; Rao *et al.*, 2010). An equal volume of plasmid DNA (1 mg/mL) was mixed with 2X DOTAP:cholesterol to form the final plasmid DNA-Lipoplex suspended in D5W (diluent consisting of 5% dextrose in water). Empty liposomes were prepared by diluting stock DOTAP:cholesterol in D5W to a final concentration of 1X. Prepared lipoplexes were stored in sterile vials at +2°C–8°C in a dark container, until ready for use. Lipoplexes were tested for sterility, endotoxin, and optical characteristics (optical density 400, particle size, and zeta potential) before final release.

Antitumor efficacy

In one study, 5- to 6-week-old female athymic nude (Hsd:Athymic Nude-*Foxn1*^{nu}) mice (Harlan Laboratories) were used as hosts for CCL-247 xenograft studies and housed in an animal facility approved by the Institutional Animal Care and Use Committee (IACUC) at University of North Texas (UNT), Health Science Center. CCL-247 cells were cultured in McCoy's medium (Hyclone; Thermo Scientific) containing 10% fetal bovine serum (Hyclone) and incubated in 5% carbon dioxide at 37°C. Tumor xenografts were established by injecting 10×10^6 CCL-247 cells subcutaneously in the right flank of mice.

Determinations on low-passage tumorgrafts derived from patient tumor were performed with athymic nude mice bred from an internal breeding colony (established from mice purchased from Charles River). The animals were housed in an animal facility approved by IACUC at Van Andel Research Institute (VARI). The tumor models in the Human Tumor Xenograft Bank at VARI were established by grafting tumor biopsy specimens from patients diagnosed with cancer into immune-compromised mice. These tumors are henceforth referred to as "tumorgrafts" to differentiate them from "tumor xenografts" established using tumor cell lines grown *in vitro*. The resulting tumorgrafts were subsequently cryopreserved and profiled molecularly on the Human Genome U133 Plus 2.0 Array (Affymetrix). Genomic analyses were performed using Xenobase-BioIntegration Solutions, a bioinformatics package developed at VARI to manage and analyze data across molecular, cellular, preclinical, and clinical platforms (www.xbtransmed.com). Primary osteosarcoma or melanoma tumor passaged in immune-compromised mice was minced into pieces and each piece was surgically implanted into athymic nude study mice subcutaneously at VARI according to the established protocol. Mice were randomly assigned to various treatment groups after tumorgraft implantation.

Mice were intratumorally injected when the tumors reached an approximate size of 100 mm^3 (CCL-247 tumor xenografts), 260 mm^3 (osteosarcoma tumorgrafts), and 160 mm^3 (melanoma tumorgrafts). IT injections were performed either singly or at 3 or 6 consecutive days or semi-weekly for 3 weeks. pbi-shSTMN1-LP was administered at doses ranging from 0.007 to 92 μg (depending on the study) in total volumes ranging from 100 to 200 μL. Controls included lipoplex containing a scrambled (sc) control, empty liposomes without plasmid DNA, and diluent (D5W:

water + 5% dextrose) administered in equivalent volumes. The tumors (either xenograft or tumorgrafts) were measured using Vernier calipers postinjection when they became palpable. Tumor volumes were calculated with the following formula: $(L \times W^2) \times 0.5$, where L is length and W is width of the tumor. All mice were monitored and tumors were measured on alternate days. Tumors were harvested and weighed on the day of sacrifice. A major part of each tissue was snap frozen in dry ice (for molecular analysis) and a small tissue piece immersed in 10% buffered formalin. The formalin-fixed tissue was paraffin embedded and hematoxylin and eosin (H&E)–stained slides were prepared. Histopathology analysis was performed by Propath Labs (mouse tumor tissues) and by IDEXX laboratories (mouse organ tissues). Assessments were based on comparisons of area distribution of viable versus necrotic areas of H&E-stained specimens by standard histopathologic criteria.

In the melanoma tumorgraft model, tumor growth progression to a surrogate endpoint was analyzed using a Kaplan–Meier estimator (Rouleau *et al.*, 2008). The surrogate endpoint was a melanoma tumorgraft size of 420 mm^3 (a size that was 50% of the average tumor size for the D5W group at the time of sacrifice).

Toxicology analysis

Six- to 7-week-old male and female Sprague–Dawley rats (Harlan Laboratories) were housed in an animal facility approved by the IACUC at UNT, Health Science Center. The animals were divided into five treatment cohorts of 60 rats (30 male and 30 female) each. Three groups were given pbi-shSTMN1-LP at one of three doses—1, 10, and 100 μg in a total volume of 300 μL. Two groups served as controls and were injected with either empty liposomes or D5W. A 5 mM DOTAP:cholesterol formulation in D5W was used for DNA encapsulation or tested as empty-liposome control at the equivalent test volume used to encapsulate 100 μg of pbi-shSTMN1. Rat body weight was measured once every week for the duration of the study. Ten rats (five male and five female) from each group were sacrificed at one of six time-points (days 2, 7, 14, 30, 60, or 90) posttreatment, and blood and internal tissues were harvested. Blood was collected for toxicology analysis: complete blood count (white blood cells [total and differential], red blood cell count, hemoglobin concentration, hematocrit, platelet counts, mean corpuscular volume, mean corpuscular hemoglobin concentration, and mean corpuscular hemoglobin), serum chemistry (alanine aminotransferase [ALT], aspartate aminotransferase [AST], creatinine, blood urea nitrogen, bilirubin, creatinine kinase, albumin, electrolytes, alkaline phosphatase, and glucose), and coagulation tests. Formalin-fixed, paraffin-embedded tissues were sectioned and H&E stained for histopathology analysis (Animal Resource Center at UT Southwestern Medical Center). Blood work analysis was performed by Comparative Clinical Pathology Lab at Research Animal Diagnostic Laboratory. Histopathology analysis of rat tissues was performed by the Cardiovascular Pathology Laboratory, Texas A&M University.

Immunoblotting

Immunoblotting was performed on frozen CCL-247 tumor xenografts treated with either pbi-shSTMN1-LP or D5W as outlined earlier (Rao *et al.*, 2010). Briefly, for each particular experiment, lysates were diluted to the same protein concentration (25 μg protein per well) and denatured via addition of β-mercaptoethanol–containing Laemmli sample buffer (Bio-Rad) and incubation at 100°C for 5 min. Western blot was performed using 10% Tris-HCl gel (Bio-Rad). The primary antibody was a mouse monoclonal antibody to human STMN1 (Opt18 E3) (sc-55531, 1:1000) or β-actin (sc-47778, 1:100,000) (Santa Cruz Biotech). The secondary antibody was horseradish peroxidase–conjugated goat antibody to mouse IgG (sc-2005, 1:2500; Santa Cruz Biotech). Development was done using the chemiluminescence detection kit (SuperSignal® West Dura Extended Duration Substrate; Thermo Scientific). Band quantification was done using G:Box software (Syngene). STMN1 protein values were normalized relative to β-actin values for each sample. Total STMN1 knockdown for each xenograft sample was determined relative to untreated CCL-247 cells cultured *in vitro*.

Detection of mature shRNA by stem-loop RT-qPCR

Frozen osteosarcoma tumorgraft samples (~30–60 mg) were homogenized for extraction of total RNA (including miRNA and shRNA) using mirVana (Ambion). Isolated total RNA was quantified using the NanoDrop spectrophotometer (Thermo Scientific). Three micrograms of total RNA was reverse transcribed in 40 μL final volume to produce cDNA using SuperScriptIII kit (Invitrogen) and guide strand–specific stem-loop reverse transcription (RT) primer (5′ GTCGTATCCAGTGCAGGGTCCGAGGTATTCGCACTGGA TACGACAAGGCA 3′). One microliter of synthesized cDNA (from 75 ng of total RNA) was used as template in the quantitative polymerase chain reaction (qPCR) with the primer pairs 5′ GCCCTTTGGCAGCCATTTG 3′ and 5′ GTGCAGGGTCCGAGGT 3′. The quantity of qPCR amplicon was measured using SYBR green fluorescent dye (Bio-Rad). A serial dilution of plasmid C10-421 (a plasmid construct containing the final 59 bp amplicon) was used in the qPCR to create the standard curve. The assay sensitivity was established at 100 copies of mature shRNA to exclude false-positive results that could result from nonspecific amplification.

Statistical analysis

All posttreatment tumor measurements were normalized to pretreatment values for individual tumors to enhance intergroup comparative analyses. Two-tailed Student's *t*-test analyses were used to compare percentage (%) of tumor growth reduction and tumor weights at necropsy between pbi-shSTMN1–treated group and D5W-treated cohort. All data analyses for the toxicology study were performed using SPSS 13.0 software (SPSS, Inc.). Differences in rat body weights and various complete blood count and serum chemistry parameters were analyzed at specific time points (days 2, 7, 14, 30, 60, and 90) or within a dose group by one-way analysis of variance. *Post hoc* comparisons were made using the Tukey test to identify specific groups varying in these parameters. For histopathology analysis for toxicology study, all morphologic diagnoses were reduced to a grouped value for each target tissue (normal, minimal/mild, moderate, or severe); then statistical analyses were performed using Kruskal–Wallis analysis of variance (two-tailed, Chi-square analysis for nonparametric data). Time to tumor growth

progression was analyzed using a Kaplan–Meier estimator (SPSS 13.0).

Results

CCL-247 tumor xenograft growth reduction by single IT treatment with pbi-shSTMN1-LP

The pbi-shSTMN1 plasmid comprises DNA encoding for STMN1-targeting bi-shRNAs that is inserted into the *SalI* and *BglII* sites of the pUMVC3 expression vector under the control of an enhanced (pol II) CMV promoter (Pizzorno *et al.*, 1988) and has been extensively characterized with respect to its biochemical features (Rao *et al.*, 2009). We observed >90% depletion of the targeted STMN1 protein in lipofected CCL-247 human colorectal cancer cells, with corresponding growth inhibition of >80% at 48 h. pbi-shSTMN1 plasmid was similarly effective in inhibiting the growth of human breast cancer (MDA-MB-231) and melanoma (SK-MEL-28) cells by 45% and 48%, respectively (data not shown). Both MDA-MB-231 and SK-MEL-28 are known to carry missense p53 mutations (Bartek *et al.*, 1990; Girnita *et al.*, 2000). Thus, the pbi-shSTMN1 vector was highly effective for inhibiting the growth of human cancer cells with wild-type or mutant p53.

Initial *in vivo* efficacy assessments were performed following a single IT injection of the lipoplexed pbi-shSTMN1 on previously established CCL-247 xenografts (Fig. 1a). We observed significant reductions of CCL-247 xenograft growth of 44% at day 7 and 55% at day 8 postinjection with 8 μg of pbi-shSTMN1-LP when compared with untreated tumors ($p < 0.05$, $n = 5$). Control expression plasmid lipoplex (scrambled LP) did not significantly alter xenograft growth (Fig. 1a). Thus, a single IT treatment of 8 μg of pbi-shSTMN1-LP was effective to achieve tumor reduction for >7 days.

Prolonged growth inhibitory activity through repeat IT treatments with pbi-shSTMN1-LP in CCL-247 tumor xenografts

To optimize antitumor efficacy through repeat injections, CCL-247–xenografted mice were treated with three daily doses of pbi-shSTMN1-LP after tumors reached a size of $\geq 100\,mm^3$. Compared with the earlier study wherein animals received only a single injection of the same dose, significant growth reductions were extended to 26 days after first injection in the 7 μg treatment arm (40% reduction; $p < 0.05$, $n = 8$), indicating that repeat treatment likely prolonged antitumor activity (Fig. 1b). Although dose-dependent outcomes were observed from 0.007 to 7 μg (0%–57% reductions at day 15 after first injection; $R^2 = 0.86$, linear regression analysis) (Fig. 2), only 7 and 34 μg treatments consistently attained significant growth reductions (57% and 48% reduction at day 15, respectively; $p < 0.05$, $n = 8$). Treatments with 0.01 μg ($p = 0.6$), 0.07 μg ($p = 0.34$), and 0.7 μg

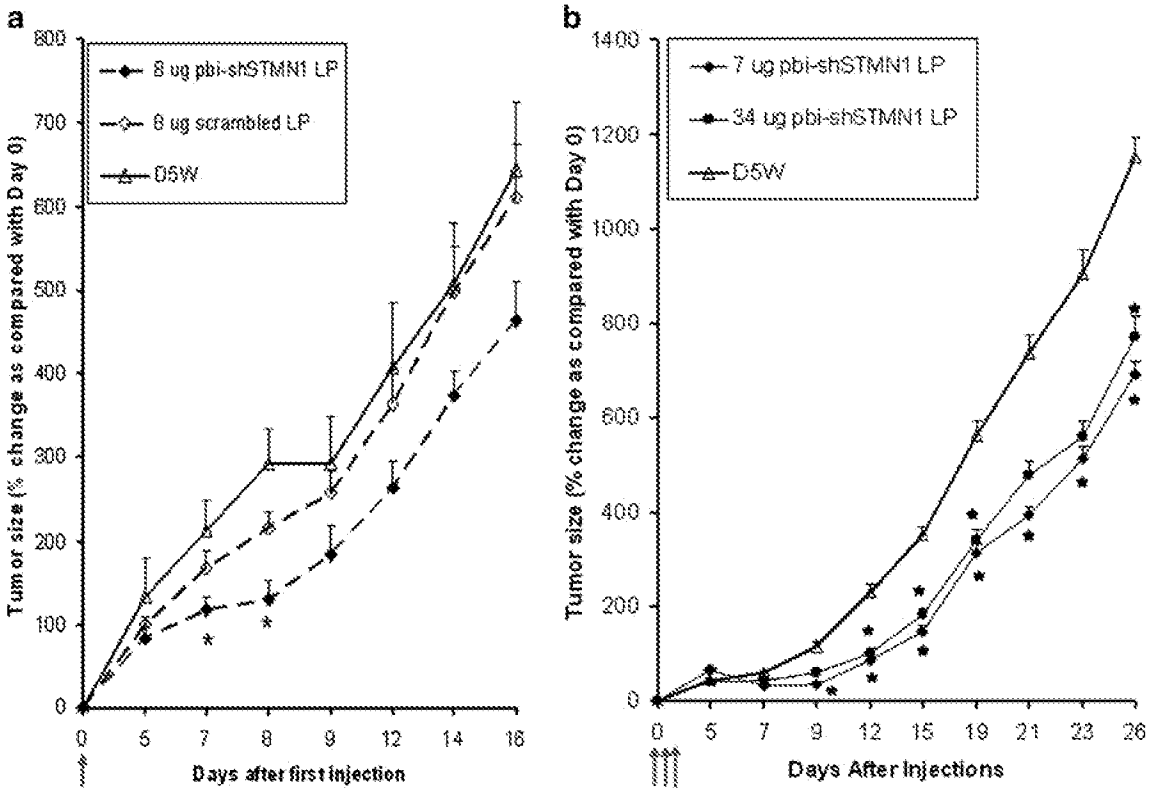

FIG. 1. CCL-247 xenograft growth inhibitory activity following IT injection of pbi-shSTMN1-LP. **(a)** CCL-247 (8×10^6 cells) tumor xenografts in athymic nude mice were injected once intratumorally. Values represent mean ± SEM ($n = 5$ for each group). Red arrow indicates injection day. *$p < 0.05$ by Student's *t*-test, compared with D5W cohort. **(b)** In a second study, CCL-247 (1×10^7 cells) tumor xenografts in athymic nude mice were injected once daily for 3 consecutive days. Values represent mean ± SEM ($n = 8$ for each group). Prolonged tumor growth reduction by pbi-shSTMN1-LP up to day 26 after first IT injection. Red arrows indicate injection days. *$p < 0.05$ by Student's *t*-test, compared with D5W cohort. IT, intratumoral; pbi-shSTMN1-LP, bi-functional shRNA specific for STMN1; SEM, standard error of mean.

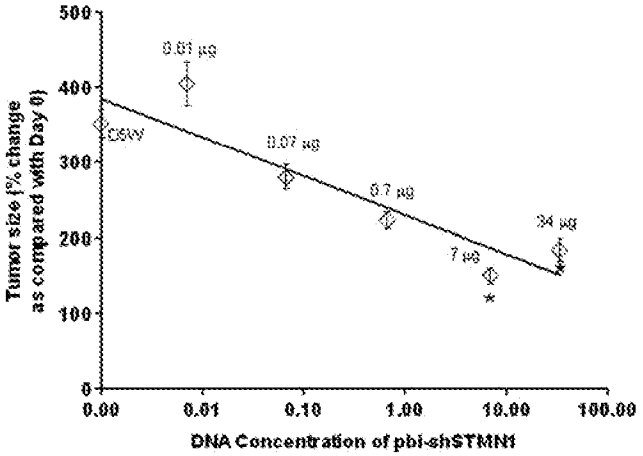

FIG. 2. Dose-dependent inhibitory activity of pbi-shSTMN1-LP using CCL-247 tumor xenografts. CCL-247 tumor xenografts in athymic nude mice were injected once daily for 3 consecutive days. Values represent mean ± SEM on day 15. CCL-247 tumor xenografts were injected with 0.01, 0.07, 0.7, 7, and 34 µg pbi-shSTMN1-LP or with diluent (D5W) ($n = 8$ for each group). Diluent (D5W)-treated tumors attained 352% of its original size at day 15. *$p \leq 0.05$.

($p = 0.07$) did not significantly alter tumor growth. These findings were confirmed by tumor weight measurements on day 26 after the first injection, with significant reduction in tumor weight for animals treated with 34 µg (0.65 ± 0.17 g; $p = 0.03$) and 7 µg (0.67 ± 0.13 g; $p = 0.04$) pbi-shSTMN1-LP when compared with D5W controls (1.00 ± 0.07 g).

In vivo *knockdown of targeted STMN1*

To confirm the *in vivo* molecular impact of pbi-shSTMN1-LP treatment, we examined STMN1 expression in harvested control and treated CCL-247 xenografts by immunoblot analysis. Cell lysates prepared from *in vitro* cultured CCL-247 cells were used as a reference control for the immunoblots. STMN1 expression in cell lysates from treated tumors was compared with protein concentration–matched samples of excised mock-treated tumors at 24 h after six consecutive IT injections (Fig. 3a, b). pbi-shSTMN1-LP–treated tumors displayed significantly reduced STMN1 expression (44%–49%; 44% median reduction when compared with untreated CCL-247 cells; 3/3 tumors tested), according to densitometric measurements normalized to β-actin expression. In contrast, D5W-treated cohorts treated with LPs with a scrambled bi-shRNA–encoding plasmid payload did not show any significantly depleted STMN1 in the representative immunoblot (Fig. 3a).

Antitumor efficacy of pbi-shSTMN1-LP in low-passage primary tumorgrafts

Recent studies showed that heterotransplanted primary human tumors can serve as clinically relevant models of investigation as they resemble the originating tumor in terms of pathology, tumor marker expression, interaction of tumor and stromal cells, and signal transduction pathways (Fu *et al.*, 1992; Perez-Soler *et al.*, 2000; Lopez-Barcons, 2009; Ding *et al.*, 2010). Tumor models established from primary human pancreatic cancer, gastrointestinal stromal tumor, and glioblastoma multiforme were more correlative predictors with respect to clinical efficacy of novel cancer therapeutics (Fu *et al.*, 1992; Lopez-Barcons, 2009; Revheim *et al.*, 2009).

To this end, confirmatory *in vivo* antitumor efficacy studies on pbi-shSTMN1-LP were performed with low-passage primary tumorgrafts derived from surgically excised human melanoma and osteosarcoma tumors generated at VARI. Based on our findings of improved tumor efficacy of repeat injections in CCL-247 xenografts, six IT treatments of pbi-shSTMN1-LP were administered to the primary melanoma tumorgraft PTSH-0021 semiweekly for 3 weeks because of slow growth rate of the tumor (Fig. 4a). pbi-shSTMN1-LP (8 µg) significantly reduced tumor growth from day 20 (41%, $p \leq 0.05$, $n = 7$) to 34 (53%, $p < 0.05$) after first injection. An increased dose of 40 µg attained stronger growth inhibition (70% reduction when compared with mock-treated tumors, $p < 0.05$ on day 26, $n = 8$) that was extended to day 46 (Fig. 4a). By comparison, similar treatments at 0.8 µg produced measurable tumor size reductions, which did not significantly differ from mock-treated tumors (33% at day 34 after first injection) or from treatments by empty liposome without an expression plasmid load (23% at day 34 after first injection). Tumor weight determinations confirmed that treatment with 40 µg pbi-shSTMN1-LP only significantly reduced tumor mass (0.46 ± 0.07 g; $p = 0.02$) when compared with D5W controls (0.85 ± 0.11 g) on the day of necropsy (day 46 after the first injection). Significantly reduced tumor mass was not observed after treatments with 0.8 or 8 µg pbi-shSTMN1-LP (0.56 ± 0.13 and 0.55 ± 0.06 g, respectively). The effect on tumor suppression at the 40 µg dose appeared most significant during the time of treatment (i.e., between days 0 and 20).

Kaplan–Meier analysis demonstrated that the median time taken by animals treated with control reagents to reach a tumor size of 420 mm^3 (surrogate indicator) was 34 and 36 days (empty liposome and D5W groups, respectively), compared with 40 days for the animals treated with the lower doses (0.8 and 8 µg pbi-shSTMN1-LP). In contrast, the median time for the 40 µg group was not reached, as only 25% of the animals reached the surrogate endpoint, hence demonstrating a marked improvement over the controls ($p < 0.001$) (Fig. 4b).

In another study using osteosarcoma tumorgrafts, six injections of 46 and 92 µg of pbi-shSTMN1-LP essentially abrogated the growth ($p < 0.05$, $n = 8$) when compared with mock-treated tumorgrafts for up to 22 days after the first injection (16 days after last injection) (Fig. 4c). The last evaluable statistical time point was day 22 after the first injection in accordance with the maximum tumor size of the control cohort before termination of study, as outlined in the study protocol.

Extended bioactivity of pbi-shSTMN1

To correlate *in vivo* efficacy with intracellular expression of bi-shSTMN1, a time course determination was carried out to identify the presence of mature shRNA effector transcripts in treated osteosarcoma tumorgrafts (Fig. 5). Tumor tissues harvested from animals that were sacrificed from days 11, 20, and 22 after first injection (equivalent to 5, 14, and 16 days after last IT injection) all displayed mature, effector shRNAs,

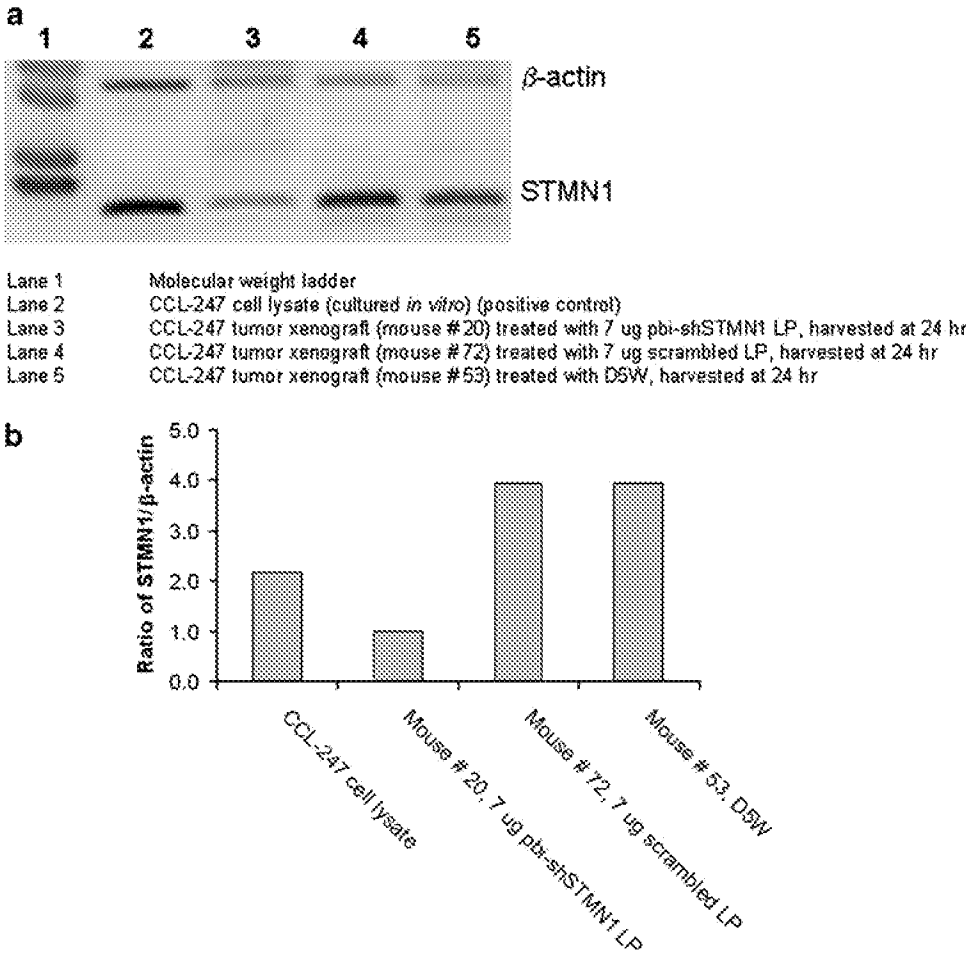

FIG. 3. *In vivo* STMN1 expression following pbi-shSTMN1-LP treatment in CCL-247 tumor xenografts. **(a)** Immunoblot analysis representing STMN1 protein in CCL-247 tumor xenografts treated IT with 7 μg pbi-shSTMN1-LP, 7 μg scrambled LP, or D5W IT on 6 consecutive days. Animals were sacrificed at 24 h after the last injection and tumors were harvested for analysis. β-Actin expression in both D5W-treated as well as pbi-shSTMN1-LP–treated samples fell within the range of 3×10^6 to 5×10^7 optical density units. Protein lysate from *in vitro* cultured CCL-247 cells was analyzed in parallel (representative one of three immunoblot analyses). **(b)** Densitometric quantification of gel image in **(a)**, following *in vivo* pbi-shSTMN1-LP treatment. Values are ratios of STMN1 to β-actin expression from harvested tumors or *in vitro* cultured CCL-247 cells (reference control).

according to stem-loop RT-qPCR determinations with sequence-specific primer/probes (Fig. 5). Seven of eight treated tumors that were harvested between days 23 and 82 after first injection (corresponding to 17 and 76 days after last injection, respectively) did not contain detectable levels of shRNA. Thus, one of three animals treated with 92 μg of pbi-shSTMN1 demonstrated detectable copies of shRNA at day 54 after first injection (i.e., day 48 after last injection) (Fig. 5).

As expected, tumors treated with scrambled LP, D5W, and empty liposomes did not display detectable levels of mature shRNA (data not shown). The extended expression of bi-shSTMN1 (up to day 16 after last injection) is an explanation for the prolonged antitumor activity of this treatment approach.

Histopathological assessments were performed on necropsied osteosarcoma tumorgrafts. Overall, residual tumorgrafts after pbi-shSTMN1-LP treatment (in either 46 or 92 μg cohorts) displayed reduced viability (mean value of 50%) when compared with tumorgrafts treated with the scrambled control (mean viability of 75%) and untreated tumors (mean viability of ~95%). There were no distinguishing, treatment-related histopathological indications in any of the major mouse organ tissues examined (Table 1).

Systemic safety analysis in immunocompetent rats, a biorelevant model of human STMN1 knockdown

We have confirmed that rats are a biorelevant model for the purpose of toxicological determinations of pbi-shSTMN1-LP, based on observations that pbi-shSTMN1-LP knocked down rat STMN1 in rat cancer cell lines. In addition, a truncated rat sequence containing the bi-shSTMN1 target sequence was transiently transfected into CCL-247 cells and knocked down by pbi-shSTMN1-LP (data not shown). Cohorts of 60 healthy rats (30 males and females, each) received pbi-shSTMN1-LP (1.0, 10, or 100 μg; murine equivalent doses of 0.26, 2.6, and 26.5 μg, respectively) by a single IV injection and were sacrificed at graded time points (days 2, 7, 14, 30, 60, or 90). pbi-shSTMN1-LP was well tolerated at doses of 1.0 and 10 μg. However, 1 of 60 ani-

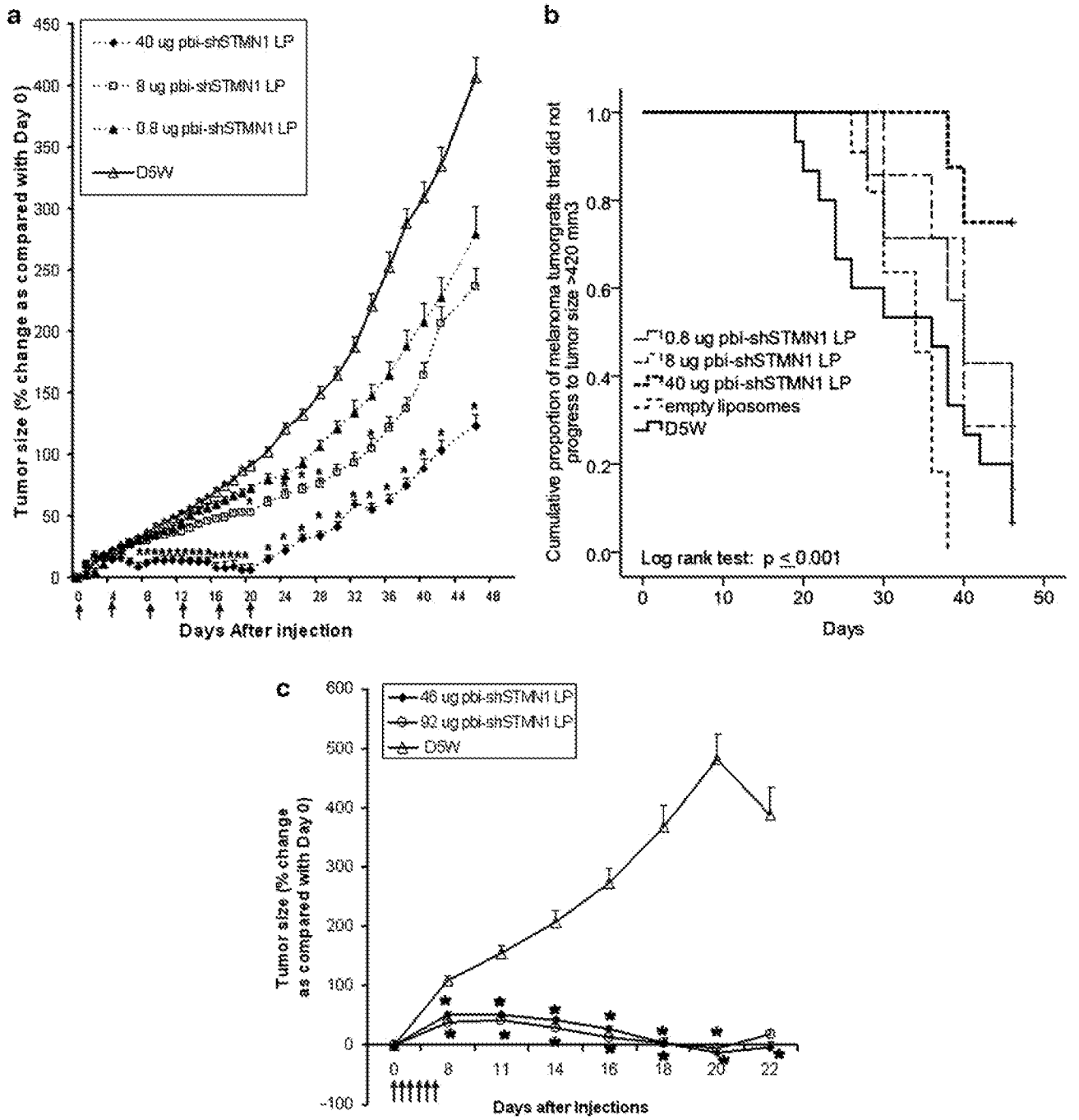

FIG. 4. Antitumor activity of pbi-shSTMN1-LP against low-passage human tumorgrafts. **(a)** Melanoma tumorgrafts were injected on a semiweekly basis for 3 weeks. Red arrows indicate injection days. Significant reduction by pbi-shSTMN1-LP was extended to day 46 after the first IT injection for the 40 μg dose group. Values represent mean ± SEM ($n = 7$ or 8 for treatment group; $n = 15$ for control (D5W)-treated group). *$p < 0.05$ by Student's t-test, compared with D5W cohort. **(b)** Kaplan–Meier analysis demonstrates increase in time to reach the surrogate melanoma tumorgraft size of 420 mm^3 (50% the average tumor size of D5W-treated group on the day of sacrifice) for the 40 μg dose group ($p < 0.001$) ($n = 7$ or 8 for treatment group; $n = 15$ for control [D5W] group; $n = 11$ for empty-liposome group). **(c)** Osteosarcoma tumorgrafts were treated with daily IT injections of pbi-shSTMN1 or control on 6 consecutive days. Values represents mean ± SEM ($n = 7$ or 8). *$p < 0.05$ by Student's t-test, compared with D5W cohort. Red arrows indicate injection days.

mals treated with pbi-shSTMN1-LP at a dose of 100 μg expired within 24 h of injection. Fifteen of the remaining 59 surviving rats demonstrated behavioral changes, which resolved by 24 h. None of the surviving rats demonstrated any toxicity beyond 24 h, and there were no histopathological changes in major organs at subsequent time points. As expected, treatment with the empty-liposome delivery vehicle also did not produce toxicity. Rat body weights were not significantly affected by any of the treatment doses of pbi-shSTMN1-LP.

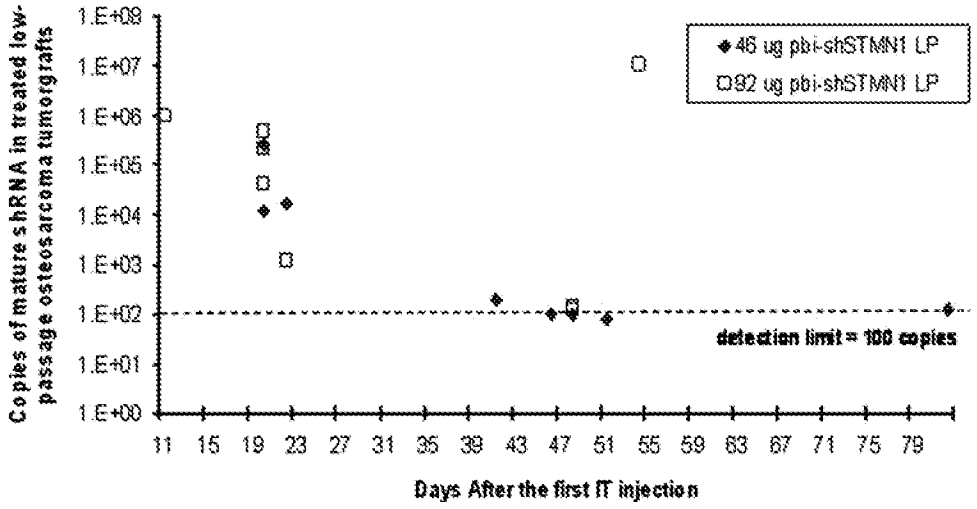

FIG. 5. Mature shRNA expression in osteosarcoma tumorgrafts treated with 46 μg pbi-shSTMN1-LP ($n=8$) or 92 μg pbi-shSTMN1-LP ($n=7$). Each symbol corresponds to expression in a single animal. Detection limit of the assay was established at 100 copies. shRNA, small hairpin RNA.

Hematologic analyses confirmed an absence of acute or chronic toxicity by pbi-shSTMN1-LP. There was neither remarkable dose- nor time-dependent alterations for coagulation time, electrolyte levels, levels of glucose, or liver enzymes, or kidney function measurements (creatinine, urea nitrogen, and creatine kinase). We observed isolated elevations in creatine kinase levels at day 90 for the highest dose group (100 μg pbi-shSTMN1-LP, $n=4/10$ vs. D5W, $n=0/10$) and elevated AST levels for the lowest dose group (1 μg pbi-shSTMN1-LP, $n=10/10$ vs. D5W, $n=0/10$) at day 14. However, there were no correspondences of abnormal AST to ALT values in these animals.

A transient reduction in platelet counts was observed at day 2 for the 100 μg pbi-shSTMN1-LP–treated group ($n=9/9$), which returned to within normal range at later time points. Complete blood counts were otherwise within the normal reference range and did not significantly differ in any of the treatment groups.

Similarly, there were no consistent and remarkable histological changes to indicate treatment-related adverse events, based on microscopic examination of potential target organs (lungs, heart, kidneys, and skeletal muscle) as identified by previously conducted biodistribution studies (Templeton *et al.*, 1997). Gross and histological changes identified in nontarget organs were sporadic, were infrequent, and could not be attributed to treatment or a particular dose. Thus, systemic injection of pbi-shSTMN1-LP fell within established safety tolerance for the observed time points. These cumulative gross toxicity and histopathologic findings indicate that the maximum tolerated dose (MTD) for administration of a single IV pbi-STMN1 LP injection was ≤100 μg (mouse equivalent of <26.5 μg; human equivalent dose (HED) of <0.09 mg/kg).

Discussion

RNAi technology has fueled the quest for personalized cancer therapy with its potential for high-throughput target identification and therapeutic application. There are currently at least 14 programs in various phases of clinical testing that are using RNAi methodology to achieve gene inhibition for various disease conditions (Vaishnaw *et al.*, 2010). Among them, hepatic and extra-hepatic cancers (three programs) and chronic myelogenous leukemia (CML) (one program) are being targeted via systemic siRNA administration.

As a parallel RNAi-based technology, we have produced an expression plasmid–based bifunctional shRNA construct specific for STMN1, which is comprised of dual stem-loop structures to simultaneously generate two functionally distinct effector small RNAs (Wu *et al.*, 2008). The pbi-shSTMN1 uses a miR30 backbone to navigate the intrinsic miRNA biogenesis process (Zeng *et al.*, 2005) and is cloned into an expression plasmid under the control of an RNA pol II promoter (Lagos-Quintana *et al.*, 2003; Lee *et al.*, 2004). One

Table 1. Histopathological Assessment for Osteosarcoma Study

Treatment group and dose	*Number of animals, n*	*Tumor as percentage of total volume (%)*	*Tumor viability (%)*	*Inflammatory infiltrate*	*Stromal response*
pbi-shSTMN1-LP (46 μg)	8	>95	50	Mild, histiocytic	Mild
pbi-shSTMN1-LP (92 μg)	8	>95	50	Mild, histiocytic	Mild
Scrambled LP (46 μg)	8	>95	70	Mild, histiocytic	Mild
Scrambled LP (92 μg)	8	>95	80	Mild, histiocytic	Mild
Empty liposomes	7	>95	90	Minimal, histiocytic	Minimal
Diluent (D5W)	7	>95	90	Minimal	Minimal

shRNA contains matched stem sequences to promote Ago2-mediated passenger-strand cleavage, and the second shRNA has a partially mismatched stem sequence to promote cleavage-independent passenger-strand departure. Thus, functionality of the effectors is set by programmed passenger-strand–guided RNA induced silencing complex (RISC) loading rather than Ago subset distribution in the cancer cell. pbi-shSTMN1 achieved effective target knockdown with a significant dose advantage in tumor cell killing *in vitro* when compared with conventional STMN1-targeting shRNAs and siRNAs. Silencing of target gene expression was more effective, with a more rapid onset and greater durability of effect (Rao *et al.*, 2010).

An effective gene-based therapeutic approach requires a platform that is effective and specific for systemic delivery of therapeutic doses of the agent to primary and metastatic tumor foci. Our liposomal delivery system incorporates a manually extruded formulation of DOTAP and cholesterol (Templeton *et al.*, 1997) that forms bilamellar invaginated vesicles (BIVs) and encapsulates the expression plasmid. At the systemic level, enhanced homing to the targeted organ site by BIV is attributed to the enhanced permeation and retention effect in inflammatory sites and solid tumors in which the vasculature, particularly the larger endothelial junction, is leaky (Tong *et al.*, 2009). BIV-encapsulated nucleic acids form flexible nanoplexes of 200–450 nm that penetrate the capillary fenestra of the tumor microenvironment as well as other tight intercellular junctions by virtue of their pliability. BIV complexes that are 200–450 nm in size have attained the highest levels of gene expression documented in all tissues and organs post–IV injections in mice (Ramesh *et al.*, 2001; Templeton, 2002, 2009). Further, the liposomal BIV complexes are fusogenic, thereby bypassing endocytosis-mediated DNA cell entry that otherwise leads to nucleic acid degradation (Simberg and Barenholz, 2005) and TLR-mediated off-target effects. Patients with end-stage lung cancer have been given multiple IV infusions of DOTAP/cholesterol 3p FUS1 gene therapy without toxicity (Lu *et al.*, 2007), and a unique DOTAP/cholesterol GNE gene lipoplex has been delivered via intramuscular and IV injection to a patient with hereditary inclusion body myopathy (HIBM2), a rare autosomal recessive neuromuscular disorder (Jay *et al.*, 2008; Phadke *et al.*, 2009; Nemunaitis *et al.*, 2010).

Previously, Mistry and coworkers have demonstrated that ribozyme- and siRNA-based STMN1 posttranscriptional knockdown reduced human prostate cancer cells *in vitro* (Mistry *et al.*, 2007; Mistry and Atweh, 2006) and osteosarcoma tumorigenicity *in vivo* (Wang *et al.*, 2007). Our present observations of *in vivo* STMN1 knockdown and growth inhibition by pbi-STMN1 extend these findings to CCL-247 colorectal cancer xenografts, illustrating the applicability of this approach to preexisting human tumors.

With respect to the CCL-247 model, the benefit of repeat injections likely stem from introduction of pbi-shSTMN1 to previously untransfected tumor cells, given that an ~5-fold increase in dose (from 7 to 34 μg) did not increase antitumor outcome. We observed marked STMN1 protein reduction in the treated tumor xenografts at 24 h after the last IT injection, confirming functionality of the pbi-shSTMN1-LP. Similar to our protein knockdown results, Huang *et al.* observed significant claudin-3 protein reduction at 3 days after the fourth IT injection (day 13 after first IT injection) of lipidiod/CLDN3 siRNA oligonucleotides into ovarian xenografts (Huang *et al.*, 2009). A detailed, separate study with earlier time-point harvests and comprehensive analysis also involving *in situ* IHC analysis as well as global molecular analysis to adequately address the causal relationship of target gene knockdown with tumor reduction is planned.

The observed *in vivo* antitumor efficacy of pbi-shSTMN1 against tumorgraft models is instructive at several levels. Our positive treatment outcome in melanoma and osteosarcoma xenografts confirms the pivotal roles of STMN1 in the pathophysiology of these tumor cell types (Clauser *et al.*, 1995; Watters *et al.*, 1998; Wang *et al.*, 2007). The significantly higher level of growth reduction with injection doses from 40 to 46 μg for these two models, not seen with the CCL-247 xenografts, may be related to a higher dependence of STMN1-related pathways in melanoma and osteosarcoma tumorgrafts (Clauser *et al.*, 1995; Watters *et al.*, 1998; Wang *et al.*, 2007). The markedly reduced viability of residual tumor mass following STMN1 knockdown confirmed our earlier *in vitro* findings and suggests that efficacy based on tumor size measurements may actually underestimate the growth inhibitory outcome of this treatment approach analogous to reported observations in the clinical ONYX-015 trials (Reid *et al.*, 2005).

A predominance of necrotic tissues within residual tumors is an explanation for the extended tumor-static findings of up to day 46 in the low-passage melanoma tumorgrafts. By comparison, duration of tumor reduction by siRNA oligonucleotide lipoplexes or naked siRNA were reported to be 4 days after second IT injection and 3 days after the last (fourth) injection in murine breast cancer syngeneic 4T1 (Tsutsumi *et al.*, 2009) and ovarian xenograft (Huang *et al.*, 2009) models, respectively. Thus, tumor growth reduction that was extended up to day 25 constituted a markedly extended treatment outcome by our bifunctional plasmid therapeutic. Correspondingly, we have demonstrated mature shRNA in pbi-shSTMN1-LP–treated low-passage osteosarcoma tumorgrafts for up to day 16 after the last IT injection based on a previously validated RT-qPCR method for miRNA (Chen *et al.*, 2005) when compared with the detectable duration of 7 days for siRNA oligonucleotides by a similar assay (Abrams *et al.*, 2010). These findings support the clinical relevance of the pbi-shSTMN1 approach, given evidence that heterotransplanted primary human tumors better resemble their clinical counterparts with respect to their biomolecular features and responsiveness to treatment, including the metastatic subset (Fu *et al.*, 1992; Perez-Soler *et al.*, 2000; Belletti *et al.*, 2008; Lopez-Barcons, 2009; Revheim *et al.*, 2009).

We performed sequential studies to demonstrate the feasibility of growth inhibition with a single injection and then to establish optimal treatment outcome with repeat injections. The initial repeat injection schemes of three or six daily injections were based on previous data by Ito *et al.* (2004) and Ramesh *et al.* (2001). Both utilized a similar DOTAP:cholesterol formulation to successfully deliver therapeutic transgenes and achieved the desired tumor growth inhibition effect. However, recent studies with liposomal (Ryschich *et al.*, 2007) or polyethylenimine (Li *et al.*, 2007; Kang *et al.*, 2009) delivery or naked siRNA (Pille *et al.*, 2005) have generated similar antitumor activity by administering IT injections two or three times weekly (three to seven total injections). On the basis of results obtained from the melanoma

and osteosarcoma tumorgraft studies, our schedule of six injections given semiweekly is considered to be the regimen of choice.

Our findings with pbi-shSTMN1-LP in biorelevant rats indicates that this nanotherapeutic is safe and well tolerated via both single or multiple IT and single IV administration. The IT MTD of >92 μg in immune-compromised mice (HED of 0.3 mg/kg) was ~10-fold higher than the extrapolated IC_{50} (9 μg, HED of 0.03 mg/kg) in the single IT treatment study with CCL-247 tumor xenografts. pbi-shSTMN1-LP demonstrated a dose-dependent efficacy, exerting maximal effect at a dose of 7–8 μg (CCL-247 tumor xenograft model) and 46 μg (low-passage melanoma tumorgraft model), respectively. At the systemic level, toxicology studies showed that the expected therapeutic dose can be safely administered, with an MTD of ≤100 μg (mouse equivalent of <26.5 μg; HED of <0.09 mg/kg). Repeat IV injections with a similar LP construct to deliver *PDX-1* oncogene-specific shRNAs have similarly led to highly effective tumor growth inhibition and survival advantage in a SCID-hu pancreatic cancer model (Liu *et al.*, 2008). Hence, the feasibility of repeat administrations with the BIV lipoplex formulation can be harnessed to achieve increased transfection efficiency and/or overcome tumor barriers (Sinek *et al.*, 2009).

Conclusion

In conclusion, we have provided proof-of-principle efficacy studies that demonstrate the feasibility of using bifunctional RNAi platform for reducing *STMN1* gene expression *in vivo*. Continuing studies aim to improve this platform in justification for targeted systemic delivery to malignant-involved areas. We have previously published successful targeted delivery of DNA products with the current delivery vehicle (Shi *et al.*, 2010) and have demonstrated successful systemic knockdown effect and survival advantage with bifunctional RNAi of other targets (i.e., *PDX-1*) with the same delivery vehicle in xenograft models (unpublished data). Our IT studies have identified the appropriate therapeutic dose for pbi-shSTMN1. Preclinical toxicology data using the bifunctional RNAi platform adds pertinent safety data to the rationale for performing IT phase I studies in cancer patients to confirm safety, document tumor effector uptake and *STMN1* downregulation, and determine the phase II recommended dose.

Acknowledgments

The authors thank Kimberly Winterrowd and Kimberly Cavanaugh at UNT Health Science Center for their assistance with animal studies. The authors gratefully acknowledge the generous support of the W.W. Caruth Jr. Foundation Fund of the Communities Foundation of Texas, the Jasper L. and Jack Denton Wilson Foundation, and the Merkle Family Foundation. The authors also thank Susan Mill and Brenda Marr for their competent assistance in the preparation of this article.

Disclosure Statement

The following authors are shareholders in Gradalis, Inc.: John Nemunaitis, Neil Senzer, Phillip Maples, Donald Rao, and Nancy Templeton. The authors have no other relevant affiliations or financial involvement with any organization or entity with a financial interest in or financial conflict with the subject matter or materials discussed in this article.

References

Abrams, M.T., Koser, M.L., Seitzer, J., Williams, S.C., DiPietro, M.A., Wang, W., Shaw, A.W., Mao, X., Jadhav, V., Davide, J.P., Burke, P.A., Sachs, A.B., Stirdivant, S.M., and Sepp-Lorenzino, L. (2010). Evaluation of efficacy, biodistribution, and inflammation for a potent siRNA nanoparticle: effect of dexamethasone co-treatment. Mol Ther **18,** 171–180.

Alli, E., Bash-Babula, J., Yang, J.M., and Hait, W.N. (2002). Effect of stathmin on the sensitivity to antimicrotubule drugs in human breast cancer. Cancer Res **62,** 6864–6869.

Alli, E., Yang, J.M., Ford, J.M., and Hait, W.N. (2007a). Reversal of stathmin-mediated resistance to paclitaxel and vinblastine in human breast carcinoma cells. Mol Pharmacol **71,** 1233–1240.

Alli, E., Yang, J.M., and Hait, W.N. (2007b). Silencing of stathmin induces tumor-suppressor function in breast cancer cell lines harboring mutant p53. Oncogene **26,** 1003–1012.

Ashihara, E., Kawata, E., and Maekawa, T. (2009). Future prospect of RNA interference for cancer therapies. Curr Drug Targets **50,** 1577–1588.

Bartek, J., Iggo, R., Gannon, J., and Lane, D.P. (1990). Genetic and immunochemical analysis of mutant p53 in human breast cancer cell lines. Oncogene **5,** 893–899.

Belletti, B., Nicoloso, M.S., Schiappacassi, M., Berton, S., Lovat, F., Wolf, K., Canzonieri, V., D'Andrea, S., Zucchetto, A., Friedl, P., Colombatti, A., and Baldassarre, G. (2008). Stathmin activity influences sarcoma cell shape, motility, and metastatic potential. Mol Biol Cell **19,** 2003–2013.

Carney, B.K., and Cassimeris, L. (2010). Stathmin/oncoprotein 18, a microtubule regulatory protein, is required for survival of both normal and cancer cell lines lacking the tumor suppressor, p53. Cancer Biol Ther **9,** 699–709.

Chen, C., Ridzon, D.A., Broomer, A.J., Zhou, Z., Lee, D.H., Nguyen, J.T., Barbisin, M., Xu, N.L., Mahuvakar, V.R., Andersen, M.R., Lao, K.Q., Livak, K.J., and Guegler, K.J. (2005). Real-time quantification of microRNAs by stem-loop RT-PCR. Nucleic Acids Res **33,** e179.

Clark, P.R., Stopeck, A.T., Ferrari, M., Parker, S.E., and Hersh, E.M. (2000). Studies of direct intratumoral gene transfer using cationic lipid-complexed plasmid DNA. Cancer Gene Ther **7,** 853–860.

Clauser, K.R., Hall, S.C., Smith, D.M., Webb, J.W., Andrews, L.E., Tran, H.M., Epstein, L.B., and Burlingame, A.L. (1995). Rapid mass spectrometric peptide sequencing and mass matching for characterization of human melanoma proteins isolated by two-dimensional PAGE. Proc Natl Acad Sci USA **92,** 5072–5076.

Ding, L., Ellis, M.J., Li, S., Larson, D.E., Chen, K., Wallis, J.W., Harris, C.C., McLellan, M.D., Fulton, R.S., Fulton, L.L., Abbott, R.M., Hoog, J., Dooling, D.J., Koboldt, D.C., Schmidt, H., Kalicki, J., Zhang, Q., Chen, L., Lin, L., Wendl, M.C., McMichael, J.F., Magrini, V.J., Cook, L., McGrath, S.D., Vickery, T.L., Appelbaum, E., Deschryver, K., Davies, S., Guintoli, T., Crowder, R., Tao, Y., Snider, J.E., Smith, S.M., Dukes, A.F., Sanderson, G.E., Pohl, C.S., Delehaunty, K.D., Fronick, C.C., Pape, K.A., Reed, J.S., Robinson, J.S., Hodges, J.S., Schierding, W., Dees, N.D., Shen, D., Locke, D.P., Wiechert, M.E., Eldred, J.M., Peck, J.B., Oberkfell, B.J., Lolofie, J.T., Du, F., Hawkins, A.E., O'Laughlin, M.D., Bernard, K.E., Cunningham, M., Elliott, G., Mason, M.D., Thompson, D.M., Jr., Ivanovich, J.L., Goodfellow, P.J., Perou, C.M., Weinstock, G.M., Aft, R., Watson, M., Ley, T.J.,

Wilson, R.K., and Mardis, E.R. (2010). Genome remodelling in a basal-like breast cancer metastasis and xenograft. Nature **464,** 999–1005.

Fu, X., Guadagni, F., and Hoffman, R.M. (1992). A metastatic nude-mouse model of human pancreatic cancer constructed orthotopically with histologically intact patient specimens. Proc Natl Acad Sci USA **89,** 5645–5649.

Gan, L., Guo, K., Li, Y., Kang, X., Sun, L., Shu, H., and Liu, Y. (2010). Up-regulated expression of stathmin may be associated with hepatocarcinogenesis. Oncol Rep **23,** 1037–1043.

Girnita, L., Girnita, A., Brodin, B., Xie, Y., Nilsson, G., Dricu, A., Lundeberg, J., Wejde, J., Bartolazzi, A., Wiman, K.G., and Larsson, O. (2000). Increased expression of insulin-like growth factor I receptor in malignant cells expressing aberrant p53: functional impact. Cancer Res **60,** 5278–5283.

Hsieh, S.Y., Huang, S.F., Yu, M.C., Yeh, T.S., Chen, T.C., Lin, Y.J., Chang, C.J., Sung, C.M., Lee, Y.L., and Hsu, C.Y. (2010). Stathmin1 overexpression associated with polyploidy, tumor-cell invasion, early recurrence, and poor prognosis in human hepatoma. Mol Carcinog **49,** 476–487.

Huang, Y.H., Bao, Y., Peng, W., Goldberg, M., Love, K., Bumcrot, D.A., Cole, G., Langer, R., Anderson, D.G., and Sawicki, J.A. (2009). Claudin-3 gene silencing with siRNA suppresses ovarian tumor growth and metastasis. Proc Natl Acad Sci USA **106,** 3426–3430.

Iancu, C., Mistry, S.J., Arkin, S., and Atweh, G.F. (2000). Taxol and anti-stathmin therapy: a synergistic combination that targets the mitotic spindle. Cancer Res **60,** 3537–3541.

Ito, I., Ji, L., Tanaka, F., Saito, Y., Gopalan, B., Branch, C.D., Xu, K., Atkinson, E.N., Bekele, B.N., Stephens, L.C., Minna, J.D., Roth, J.A., and Ramesh, R. (2004). Liposomal vector mediated delivery of the 3p FUS1 gene demonstrates potent antitumor activity against human lung cancer *in vivo*. Cancer Gene Ther **11,** 733–739.

Jay, C., Nemunaitis, G., Nemunaitis, J., Senzer, N., Hinderlich, S., Darvish, D., Ogden, J., Eager, J., Tong, A., and Maples, P. (2008). Preclinical assessment of wt GNE gene plasmid for management of hereditary inclusion body myopathy 2 (HIBM2). Gene Regul Syst Bio **2,** 243–252.

Jeon, T.Y., Han, M.E., Lee, Y.W., Lee, Y.S., Kim, G.H., Song, G.A., Hur, G.Y., Kim, J.Y., Kim, H.J., Yoon, S., Baek, S.Y., Kim, B.S., Kim, J.B., and Oh, S.O. (2010). Overexpression of stathmin1 in the diffuse type of gastric cancer and its roles in proliferation and migration of gastric cancer cells. Br J Cancer **102,** 710–718.

Jiang, L., Chen, Y., Chan, C.Y., Wang, X., Lin, L., He, M.L., Lin, M.C., Yew, D.T., Sung, J.J., Li, J.C., and Kung, H.F. (2009). Down-regulation of stathmin is required for TGF-beta inducible early gene 1 induced growth inhibition of pancreatic cancer cells. Cancer Lett **274,** 101–108.

Kang, Y., Zhang, X., Jiang, W., Wu, C., Chen, C., Zheng, Y., Gu, J., and Xu, C. (2009). Tumor-directed gene therapy in mice using a composite nonviral gene delivery system consisting of the piggyBac transposon and polyethylenimine. BMC Cancer **9,** 126.

Lagos-Quintana, M., Rauhut, R., Meyer, J., Borkhardt, A., and Tuschl, T. (2003). New microRNAs from mouse and human. RNA **9,** 175–179.

Lee, Y., Kim, M., Han, J., Yeom, K.H., Lee, S., Baek, S.H., and Kim, V.N. (2004). MicroRNA genes are transcribed by RNA polymerase II. EMBO J **23,** 4051–4060.

Li, S., Dong, W., Zong, Y., Yin, W., Jin, G., Hu, Q., Huang, X., Jiang, W., and Hua, Z.C. (2007). Polyethylenimine-complexed plasmid particles targeting focal adhesion kinase function as melanoma tumor therapeutics. Mol Ther **15,** 515–523.

Liu, S., Ballian, N., Belaguli, N.S., Patel, S., Li, M., Templeton, N.S., Gingras, M.C., Gibbs, R., Fisher, W., and Brunicardi, F.C. (2008). PDX-1 acts as a potential molecular target for treatment of human pancreatic cancer. Pancreas **37,** 210–220.

Liu, Y., and Bodmer, W.F. (2006). Analysis of P53 mutations and their expression in 56 colorectal cancer cell lines. Proc Natl Acad Sci USA **103,** 976–981.

Lopez-Barcons, L.A. (2009). Small-cell neuroendocrine carcinoma of the prostate: are heterotransplants a better experimental model? Asian J Androl **12,** 308–314.

Lu, C., Sepulveda, C.A., Ji, L., Ramesh, R., O'Connor, S., Jayachandran, G., Hicks, M.E., Munden, R.F., Lee, J.J., Templeton, N.S., McMannis, J.D., Stewart, D.J., and Roth, J.A. (2007). Systemic therapy with tumor suppressor FUS1-nanoparticles for stage IV lung cancer. In *Annual AACR Meeting*. Los Angeles, CA.

Mistry, S.J., and Atweh, G.F. (2002). Role of stathmin in the regulation of the mitotic spindle: potential applications in cancer therapy. Mt Sinai J Med **69,** 299–304.

Mistry, S.J., and Atweh, G.F. (2006). Therapeutic interactions between stathmin inhibition and chemotherapeutic agents in prostate cancer. Mol Cancer Ther **5,** 3248–3257.

Mistry, S.J., Bank, A., and Atweh, G.F. (2007). Synergistic anti-angiogenic effects of stathmin inhibition and taxol exposure. Mol Cancer Res **5,** 773–782.

Nemunaitis, G., Maples, P.B., Jay, C., Gahl, W.A., Huizing, M., Poling, J., Tong, A.W., Phadke, A.P., Pappen, B.O., Bedell, C., Templeton, N.S., Kuhn, J., Senzer, N., and Nemunaitis, J. (2010). Hereditary inclusion body myopathy: single patient response to GNE gene Lipoplex therapy. J Gene Med **12,** 403–412.

Nemunaitis, J., Senzer, N., Khalil, I., Shen, Y., Kumar, P., Tong, A., Kuhn, J., Lamont, J., Nemunaitis, M., Rao, D., Zhang, Y.A., Zhou, Y., Vorhies, J., Maples, P., Hill C., and Shanahan, D. (2007). Proof concept for clinical justification of network mapping for personalized cancer therapeutics. Cancer Gene Ther **14,** 686–695.

Nomura, T., Nakajima, S., Kawabata, K., Yamashita, F., Takakura, Y., and Hashida, M. (1997). Intratumoral pharmacokinetics and *in vivo* gene expression of naked plasmid DNA and its cationic liposome complexes after direct gene transfer. Cancer Res **57,** 2681–2686.

Olivier, M., Petitjean, A., Marcel, V., Petre, A., Mounawar, M., Plymoth, A., de Fromentel, C.C., and Hainaut, P. (2009). Recent advances in p53 research: an interdisciplinary perspective. Cancer Gene Ther **16,** 1–12.

Perez-Soler, R., Kemp, B., Wu, Q.P., Mao, L., Gomez, J., Zeleniuch-Jacquotte, A., Yee, H., Lee, J.S., Jagirdar, J., and Ling, Y.H. (2000). Response and determinants of sensitivity to paclitaxel in human non-small cell lung cancer tumors heterotransplanted in nude mice. Clin Cancer Res **6,** 4932–4938.

Phadke, A.P., Jay, C., Chen, S.J., Haddock, C., Wang, Z., Yu, Y., Nemunaitis, D., Nemunaitis, G., Templeton, N.S., Senzer, N., Maples, P.B., Tong, A.W., and Nemunaitis, J. (2009). Safety and *in vivo* expression of a GNE-transgene: a novel treatment approach for hereditary inclusion body myopathy-2. Gene Regul Syst Bio **3,** 89–101.

Pille, J.Y., Denoyelle, C., Varet, J., Bertrand, J.R., Soria, J., Opolon, P., Lu, H., Pritchard, L.L., Vannier, J.P., Malvy, C., Soria, C., and Li, H. (2005). Anti-RhoA and anti-RhoC siRNAs inhibit the proliferation and invasiveness of MDA-MB-231 breast cancer cells *in vitro* and *in vivo*. Mol Ther **11,** 267–274.

Pizzorno, M.C., O'Hare, P., Sha, L., LaFemina, R.L., and Hayward, G.S. (1988). Trans-activation and autoregulation of gene

expression by the immediate-early region 2 gene products of human cytomegalovirus. J Virol **62,** 1167–1179.

Ramesh, R., Saeki, T., Templeton, N.S., Ji, L., Stephens, L.C., Ito, I., Wilson, D.R., Wu, Z., Branch, C.D., Minna, J.D., and Roth, J.A. (2001). Successful treatment of primary and disseminated human lung cancers by systemic delivery of tumor suppressor genes using an improved liposome vector. Mol Ther **3,** 337–350.

Rana, S., Maples, P.B., Senzer, N., and Nemunaitis, J. (2008). Stathmin 1: a novel therapeutic target for anticancer activity. Expert Rev Anticancer Ther **8,** 1461–1470.

Rao, D.D., Maples, P.B., Senzer, N., Kumar, P., Wang, Z., Pappen, B.O., Yu, Y., Haddock, C., Jay, C., Phadke, A.P., Chen, S., Kuhn, J., Dylewski, D., Scott, S., Monsma, D., Webb, C., Tong, A., Shanahan, D., and Nemunaitis, J. (2010). Enhanced target gene knockdown by a bifunctional shRNA: a novel approach of RNA interference. Cancer Gene Ther **17,** 780–791.

Rao, D.D., Senzer, N., Cleary, M.A., and Nemunaitis, J. (2009). Comparative assessment of siRNA and shRNA off target effects: what is slowing clinical development. Cancer Gene Ther **16,** 807–809.

Rayburn, E.R., and Zhang, R. (2008). Antisense, RNAi, and gene silencing strategies for therapy: mission possible or impossible? Drug Discov Today **13,** 513–521.

Reid, T.R., Freeman, S., Post, L., McCormick, F., and Sze, D.Y. (2005). Effects of Onyx-015 among metastatic colorectal cancer patients that have failed prior treatment with 5-FU/leucovorin. Cancer Gene Ther **12,** 673–681.

Revheim, M.E., Seierstad, T., Berner, J.M., Bruland, O.S., Roe, K., Ohnstad, H.O., Bjerkehagen, B., and Bach-Gansmo, T. (2009). Establishment and characterization of a human gastrointestinal stromal tumour (GIST) xenograft in athymic nude mice. Anticancer Res **29,** 4331–4336.

Rouleau, C., Menon, K., Boutin, P., Guyre, C., Yoshida, H., Kataoka, S., Perricone, M., Shankara, S., Frankel, A.E., Duesbery, N.S., Vande Woude, G., Biemann, H.P., and Teicher, B.A. (2008). The systemic administration of lethal toxin achieves a growth delay of human melanoma and neuroblastoma xenografts: assessment of receptor contribution. Int J Oncol **32,** 739–748.

Rubin, C.I., and Atweh, G.F. (2004). The role of stathmin in the regulation of the cell cycle. J Cell Biochem **93,** 242–250.

Ryschich, E., Huszty, G., Wentzensen, N., Schmidt, E., Knaebel, H.P., Encke, J., Marten, A., Buchler, M.W., and Schmidt, J. (2007). Effect of Flt3 ligand gene transfer in experimental pancreatic cancer. Int J Colorectal Dis **22,** 215–223.

Shi, Q., Nguyen, A.T., Angell, Y., Deng, D., Na, C.R., Burgess, K., Roberts, D.D., Brunicardi, F.C., and Templeton, N.S. (2010). A combinatorial approach for targeted delivery using small molecules and reversible masking to bypass nonspecific uptake *in vivo*. Gene Ther **17,** 1085–1097.

Simberg, D.W.A., and Barenholz, Y. (2005). Reversible mode of binding of serum proteins to DOTAP/cholesterol Lipoplexes: a possible explanation for intravenous lipofection efficiency. Hum Gene Ther **16,** 1087–1096.

Sinek, J.P., Sanga, S., Zheng, X., Frieboes, H.B., Ferrari, M., and Cristini, V. (2009). Predicting drug pharmacokinetics and effect in vascularized tumors using computer simulation. J Math Biol **58,** 485–510.

Templeton, N.S. (2002). Cationic liposome-mediated gene delivery *in vivo*. Biosci Rep **22,** 283–295.

Templeton, N.S. (2009). Nonviral delivery for genomic therapy of cancer. World J Surg **33,** 685–697.

Templeton, N.S., Lasic, D.D., Frederik, P.M., Strey, H.H., Roberts, D.D., and Pavlakis, G.N. (1997). Improved DNA: liposome complexes for increased systemic delivery and gene expression. Nat Biotechnol **15,** 647–652.

Tong, A.W., Jay, C.M., Senzer, N., Maples, P.B., and Nemunaitis, J. (2009). Systemic therapeutic gene delivery for cancer: crafting Paris' arrow. Curr Gene Ther **9,** 45–60.

Tsutsumi, K., Yamaura, T., Nakajima, M., Honda, T., and Kasaoka, T. (2009). Silencing of focal adhesion kinase by tumor direct injection of small interfering RNA decreases *in vivo* tumor growth. Cancer Biol Ther **8,** 1292–1299.

Vaishnaw, A.K., Gollob, J., Gamba-Vitalo, C., Hutabarat, R., Sah, D., Meyers, R., de Fougerolles, T., and Maraganore, J. (2010). A status report on RNAi therapeutics. Silence **1,** 14.

Wang, R., Dong, K., Lin, F., Wang, X., Gao, P., Wei, S.H., Cheng, S.Y., and Zhang, H.Z. (2007). Inhibiting proliferation and enhancing chemosensitivity to taxanes in osteosarcoma cells by RNA interference-mediated downregulation of stathmin expression. Mol Med **13,** 567–575.

Watters, D., Garrone, B., Coomer, J., Johnson, W.E., Brown, G., and Parsons, P. (1998). Stimulation of melanogenesis in a human melanoma cell line by bistratene A. Biochem Pharmacol **55,** 1691–1699.

Wu, L., Fan, J., and Belasco, J.G. (2008). Importance of translation and nonnucleolytic ago proteins for on-target RNA interference. Curr Biol **18,** 1327–1332.

Yuan, R.H., Jeng, Y.M., Chen, H.L., Lai, P.L., Pan, H.W., Hsieh, F.J., Lin, C.Y., Lee, P.H., and Hsu, H.C. (2006). Stathmin overexpression cooperates with p53 mutation and osteopontin overexpression, and is associated with tumour progression, early recurrence, and poor prognosis in hepatocellular carcinoma. J Pathol **209,** 549–558.

Zeng, Y., Cai, X., and Cullen, B.R. (2005). Use of RNA polymerase II to transcribe artificial microRNAs. Methods Enzymol **392,** 371–380.

Zhang, H.Z., Gao, P., Yan, L., and Lin, F. (2004). Significance of stathmin gene overexpression in osteosarcoma cells. Ai Zheng **23,** 493–496.

Zhang, H.Z., Wang, Y., Gao, P., Lin, F., Liu, L., Yu, B., Ren, J.H., Zhao, H., and Wang, R. (2006). Silencing stathmin gene expression by survivin promoter-driven siRNA vector to reverse malignant phenotype of tumor cells. Cancer Biol Ther **5,** 1457–1461.

Zhang, S., Zhao, B., Jiang, H., Wang, B., and Ma, B. (2007). Cationic lipids and polymers mediated vectors for delivery of siRNA. J Control Release **123,** 1–10.

Address correspondence to:
John Nemunaitis, M.D.
Gradalis, Inc.
1700 Pacific Avenue
Suite 1100
Dallas, TX 75201

E-mail: jnemunaitis@marycrowley.org

Received for publication January 31, 2011; received in revised form March 3, 2011; accepted March 4, 2011.